

2-(3-Oxo-1,3-diphenylpropyl)malonic Acids as Potent Allosteric Ligands of the PIF Pocket of Phosphoinositide-Dependent Kinase-1: Development and Prodrug Concept

Adriana Wilhelm,[†] Laura A. Lopez-Garcia,[‡] Katrien Busschots,[‡] Wolfgang Fröhner,[†] Frauke Maurer,[§] Stefan Boettcher,[†] Hua Zhang,[‡] Jörg O. Schulze,[‡] Ricardo M. Biondi,[‡] and Matthias Engel^{*,†}

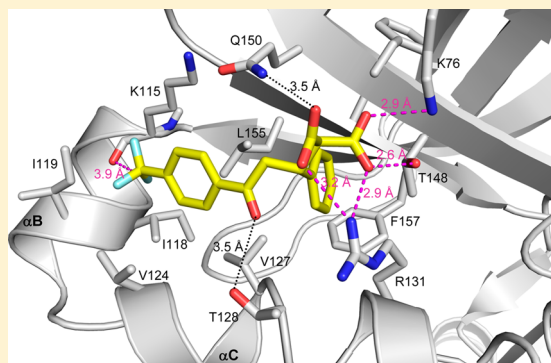
[†]Pharmaceutical and Medicinal Chemistry, Saarland University, Campus C2.3, D-66123 Saarbrücken, Germany

[‡]Department of Internal Medicine I, University of Frankfurt, Theodor-Stern-Kai 7, D-60590 Frankfurt a.M., Germany

[§]Organic Chemistry, Saarland University, Campus C2.3, D-66123 Saarbrücken, Germany

S Supporting Information

ABSTRACT: The protein kinase C-related kinase 2 (PRK2)-interacting fragment (PIF) pocket of phosphoinositide-dependent kinase-1 (PDK1) was proposed as a novel target site for allosteric modulators. In the present work, we describe the design, synthesis, and structure–activity relationship of a series of 2-(3-oxo-1,3-diphenylpropyl)malonic acids as potent allosteric activators binding to the PIF pocket. Some congeners displayed AC₅₀ values for PDK1 activation in the submicromolar range. The potency of the best compounds to stabilize PDK1 in a thermal stability shift assay was in the same order of magnitude as that of the PIF pocket binding peptide PIFtide, suggesting comparable binding affinities to the PIF pocket. The crystal structure of PDK1 in complex with compound **4h** revealed that additional ionic interactions are mainly responsible for the increased potency compared to the monocarboxylate analogues. Notably, several compounds displayed high selectivity for PDK1. Employing a prodrug strategy, we were able to corroborate the novel mechanism of action in cells.



■ INTRODUCTION

The Ser/Thr kinase phosphoinositide-dependent kinase-1 (PDK1) is a pivotal regulator constitutively phosphorylating some substrates and also acting downstream of insulin- and growth factor receptor-activated phosphatidylinositol-3 (PI3) kinase. PDK1 phosphorylates and activates at least 23 protein kinases from the AGC family.^{1,2} The PDK1 substrates, including all isoforms of p70 S6 kinase (S6K), p90 ribosomal S6 kinase (RSK), serum- and glucocorticoid-induced protein kinase (SGK), PKC isoforms, protein kinase C-related kinase 2 (PRK2), and PKB/AKT, are implicated in various cellular processes such as metabolism, cell growth, differentiation, and survival.^{2–4} Hence, constitutive activation of PDK1 can lead to cancer and other disorders including inflammation, arthritis, diabetes, and cardiovascular disease. In the past, PDK1 has been extensively investigated as an oncology target, while other potential indications have received little attention so far.

A lot of effort was dedicated to the development of inhibitors targeting the ATP binding pocket.^{5–9} However, analysis of several structural classes of small-molecule PDK1 inhibitors did not reveal any selective compound, which can be attributed to their purely ATP-competitive mechanism of action.^{10,11} Only recently, an inhibitor binding to the inactive form of PDK1 by stabilizing a DFG-out conformation in the active site was reported, which displayed a high selectivity.¹¹ Interestingly, this

type II inhibitor diminished only anchorage-independent growth and cell migration but not normal proliferation of several tumor cell lines, suggesting that the mode of action of an inhibitor can largely influence its potential therapeutic effect.¹¹ With respect to a potential application for the treatment of diabetes type 2, the requirements for a PDK1 inhibitor would be to inhibit downstream activation of substrate kinases responsible for desensitization of insulin signaling, in particular S6K,¹² while not affecting the activity of other substrates that function as downstream mediators of insulin action. Such a pharmacological profile can hardly be reached by compounds directed to the ATP binding site, which are expected to prevent the activation of all substrate kinases, including AKT/PKB. Whereas evidence from knockout studies suggests that inhibition of S6K-catalyzed phosphorylation of the insulin receptor substrate (IRS)1 might lead to attenuation of a negative feedback loop and sensitize cells to insulin,^{13–15} PKB plays a pivotal role in mediating glucose uptake and storage (reviewed in ref 16). Knockdown of PKB β caused insulin resistance and severe diabetes.¹⁶ Similarly, systemic RNAi-mediated knockdown of the PDK1 activity by 90% induced hyperglycemia and hyperinsulinemia in mice, which

Received: July 17, 2012

Published: October 29, 2012

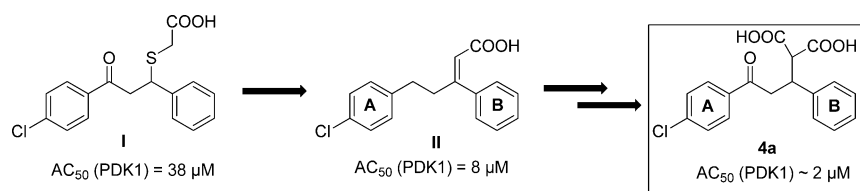


Figure 1. Design of the novel allosteric modulator **4a** based on the previous scaffolds **I** and **II**.

might be due to repression of PKB activation.¹⁷ In a further study, pancreas-specific PDK1 knockout mice developed severe hyperglycemia and pancreatic hypoplasia.¹⁸

In contrast to ATP-competitive inhibitors, allosteric ligands binding to the so-called PRK2-interacting fragment (PIF) pocket of PDK1 might allow a more selective modulation of downstream activations and hence could be explored as potential agents for the treatment of diabetes type 2. The PIF pocket is a shallow hydrophobic pocket on the small lobe of the catalytic domain, which is shared with all members of the AGC kinase family.¹⁹ In PDK1, it serves two functions: (i) as an allosteric site regulating the catalytic activity, and (ii) as a docking site for the transient interaction with the C-terminal hydrophobic motif (HM) peptides of the substrate kinases, which share the consensus core sequence F-X-X-F-S(P)/T(P)/D-Y (X: any amino acid; P: phosphate group).

Most inactive substrate kinases of PDK1 depend on binding of their C-terminal HM peptide to the PIF pocket in order to become phosphorylated and activated, according to point (ii) above.^{2,20} Therefore, compounds directed to the PIF pocket are expected to compete with the essential docking of the substrate's HM peptides, thus preventing the activation of many substrates in the insulin signaling pathway, including S6K. In this regard, PIF pocket ligands are predicted to function as inhibitors of protein–protein interactions between the PIF pocket and the HM peptides. Interestingly, the PIF pocket meets the criteria as identified by Bogan and Thorn for druggable hot spots in protein–protein interfaces, which were characterized as being enriched by hydrophobic aromatic residues, and basic residues, in particular arginine.²¹

As an important exception in the PDK1 pathway, the activation of PKB is not dependent on the PIF pocket.²⁰ Rather, the phosphorylation of PKB is triggered by colocalization with PDK1 at the membrane, mediated by binding of their pleckstrin homology (PH) domains to phosphatidylinositol (3,4,5)-trisphosphate.^{22,23} Thus, compounds directed to the PIF pocket of PDK1 should not affect the activation of PKB, compatible with a potential application for the treatment of diabetes type 2.

Of concern is rather the potential inhibition of PKC ζ , which was reported to enhance glucose transport in skeletal muscle, and its activation was shown to be impaired in diabetes type 2.^{24–26} PKC ζ is phosphorylated by PDK1 at the activation loop residue Thr410.²⁷ In agreement with the postulated PIF-pocket-dependent mechanism of activation, expression of glutathione-S-transferase (GST)-PIFtide, which competes with binding of the PKC ζ HM peptide to the PIF pocket, prevented the T-loop phosphorylation and activation of PKC ζ in HEK293 cells.²⁸ However, the phosphorylation of the PKCs by PDK1 is believed to initiate the maturation process after biosynthesis, leading to a PKC species constitutively phosphorylated at the activation loop, obviating the need for PDK1 activity at later stages of the protein life span.²⁹ So far, the effect of a short-term blocking of the PDK1 PIF pocket on

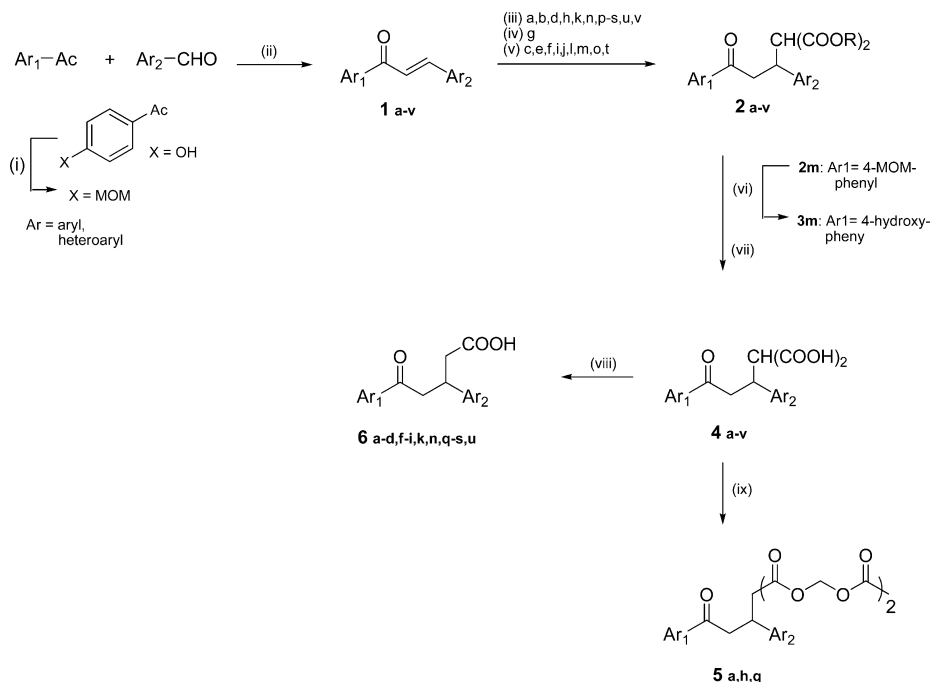
the PKC ζ phosphorylation state in intact cells was not analyzed yet.

Of note, the selective effects of PIF pocket blockage in cells as outlined above are expected to occur with any PIF-pocket ligands that are either allosteric activators or neutral antagonists with respect to the influence on catalytic activity. By contrast, allosteric inhibitors would affect the phosphorylation of all substrates, including PKB.

In our previous work, we published the first small molecules that were able to allosterically activate PDK1 by binding to the PIF pocket.³⁰ Furthermore, we described the structure–activity relationship (SAR) of a larger series of 3,5-diphenylpent-2-enoic acids as PIF-pocket-directed PDK1 activators, providing evidence that the PIF pocket might be a druggable site.³¹ The binding mode of one of these compounds and part of the allosteric mechanism were characterized by methods in solution and using X-ray analysis of a cocrystal structure with PDK1.³² Further compounds suggested to bind to the PIF pocket were discovered by other groups employing different techniques including NMR-based fragment screening, molecular docking, and ultrahigh throughput screening.^{33–35} While most small molecule PIF-pocket ligands were activators of the catalytic activity, Sadowsky et al. reported small fragments that acted as allosteric inhibitors after covalent disulfide linkage to a mutated Cys residue at the PIF-pocket border.³⁶

The affinity of the most potent HM peptide known so far, PIFtide (a 24-mer deriving from the PDK1 substrate PRK2), was determined in the range 43–90 nM (K_d value).^{30,37} However, the affinity of most reversible ligands described hitherto was rather low, in the micromolar K_d range, which appeared insufficient to effectively compete with binding of the substrate HM peptides to the PIF pocket in cells. Wei et al.³⁴ reported a series of PDK1 activators exhibiting an up to 5 times greater potency in displacing PIFtide from PDK1 protein than compound **I** (Figure 1). However, this finding was obscured by unexpectedly high AC_{50} values toward the PDK1 preparation used (>15 μ M). Thus, the potential efficacy toward native PDK1 in a cellular setting remains unclear. In addition to strong binding affinity, high selectivity is another prerequisite to perform detailed cellular and in vivo studies for a proof-of-principle; selectivity data were only reported for a few PDK1 PIF-pocket ligands hitherto. The objective of the present study was therefore to develop high affinity ligands for the PDK1 PIF pocket that were able to compete with endogenous HM peptides and that were not targeting the PIF pockets of related kinases from the AGC family. As an additional prerequisite, the effects of the PIF pocket ligands on the catalytic activity were preferred to be activating or neutral, in order to prevent inhibition of PKB.

In the following, we describe the design, synthesis, and SAR of 2-(3-oxo-1,3-diphenylpropyl)malonic acids as a new class of PDK1 activators with improved potency and high selectivity even toward closely related AGC kinases. Furthermore, the binding mode was elucidated by cocrystallography. In order to

Scheme 1. Synthetic Procedures Used to Prepare the Title Compounds^a

^aReagents and conditions: (i) bromomethyl-methylether, NaH, DME, 0 °C, 1 h; (ii) method A: NaOH, EtOH, 1 h, rt; (iii) method B1: diethyl malonate, MgO, toluene, reflux, 2 h; (iv) method B2: diethyl malonate, K₂CO₃, ethanol, reflux, 2 h; (v) method B3: diethyl malonate, NaH, methanol, reflux, 2 h; (vi) 10% HCl, methanol, reflux, 2 h; (vii) method C: NaOH, EtOH, rt, 4 h; (viii) method D: 160–170 °C, 2 h; (ix) method E: bromomethyl acetate, NEt₃, DMF, rt, 4 h. For substituents “Ar” see Table 1.

enable cellular studies, some of the highly polar compounds were converted into prodrugs. Finally, the effect of one prodrug on the phosphorylation of the PDK1 substrates S6K, PKCζ, and AKT/PKB was examined in cells.

RESULTS AND DISCUSSION

Chemistry. In order to optimize potency of previous compound series, we designed a chimeric compound retaining the ketone function from compound I combined with the shorter carboxyl side chain from compound class II (Figure 1). While the keto group offered potential for additional H-bond interaction, a further goal was to provide a better mimetic for the phosphate group, since the natural ligands of the PDK1 PIF pocket are mostly phosphopeptides. We assigned this role to the malonic acid moiety, thus yielding compound 4a. Scheme 1 depicts the synthetic route for the new compound classes.

The malonic acid derivatives were prepared starting from the previously described 1,3-(heteroaryl/aryl)-prop-2-en-1-ones (chalcones)³¹ 1a–v in three steps. These were accessible by classical Claisen–Schmidt condensation of benzaldehydes or heteroarylaldehydes with acetophenones or heteroaryl methyl ketones. The chalcones were converted to the corresponding dialkyl 2-(3-oxo-1,3-diheteroaryl-/arylpropyl)malonates via base-catalyzed Michael addition of CH-acidic malonates. Due to its mildly basic nature, magnesium oxide was used whenever possible, ensuring facile product isolation and good activity of most of the Michael adducts 2a, 2b, 2d, 2h, 2k, 2n, 2p–s, 2u, and 2v.³⁸ However, because of the limited activity depending on the solvent and the chalcone, the remaining malonate derivatives were obtained using alternative catalysts, potassium carbonate for 2g and sodium hydride for 2c, 2e–j, 2l, 2m, 2o, and 2t.^{39,40} Treatment with sodium hydride in methanol caused transesterification leading to the dimethyl intermediates.

Alkaline hydrolysis of the alkyl malonate analogues under reflux afforded the corresponding (3-oxo-1,3-diheteroaryl/arylpropyl)malonic acids 4a–v. Finally, pyrolysis of the corresponding malonic acid analogues at about 165 °C provided facile access to the 5-oxo-3,5-diheteroaryl/arylpentanoic acids 6a–d, 6f–i, 6k, 6n, 6q–s, and 6u.⁴¹ To enable cell permeation of the highly polar carboxylic acids, carrier prodrug forms were synthesized. Treatment of the (3-oxo-1,3-diheteroaryl/arylpropyl)malonic acids 4a–v with bromo methylacetate and triethylamine in dimethylformamide afforded the bis- or monoacetoxymethylester derivatives 5a, 5e, 5g–i, 5l, 5n, 5o, 5q, 5r, 7g, and 7q in modest yields.⁴²

Synthesis of 4m, starting from 4-hydroxyacetophenone, required protection of the nucleophilic alcohol function. To this end, the methoxymethyl (MOM) group was introduced using bromomethyl-methylether with sodium hydride in dimethylformamide.⁴³ Finally, the MOM group was cleaved under acidic conditions to give the desired dimethyl 2-(1-(4-chlorophenyl)-3-(4-hydroxyphenyl)-3-oxopropyl)malonate 3m followed by hydrolysis to furnish the target molecule 4m.⁴³

Biological Activity. 1,3-Diaryl Malonyl Propanones Potently Activate PDK1 via Binding to the PIF Pocket. We analyzed the effect of the malonic acid analogues on the activity of PDK1 using a radioactive kinase assay exactly as previously described.³⁰ For comparison, the effect of compound II was measured in parallel, whereby the published data³¹ were essentially reproduced (AC₅₀: 8 μM; A_{max}: 3-fold). As can be seen from Table 1, most of the dicarboxyl compounds including the most comparable analogue 4a prompted a stronger allosteric activation of PDK1 and displayed lower AC₅₀ values than II. Several analogues, comprising 4f, 4o, 4q, 4u, and 4v, were found to be even more potent under these

Table 1. Activity of the 1,3-Diaryl Malonyl Propanones and the Corresponding Monoacids towards PDK1 (Cell-Free Kinase Activity Assay)

No.	Structure ^a	A _{max} ^b fold	AC ₅₀ ^b μM	No.	Structure ^a	A _{max} ^b fold	AC ₅₀ ^b μM
4a		4.0	2.5	6a		3.0	>20
4b		2.6	4.0	6b		2.5	>70
4c		2.0	> 10	6c		n.e.	n.e.
4d		3.7	1.4	6d		2	>20
4e		3.0	12.0	-	-	-	-
4f		4.0	0.4	6f		4.0	10
4g		3.8	2.0	6g		2.5	20
4h		5.5	2.0	6h		4.0	15
4h- eutomer		5.5	1.8	-	-	-	-
4h- distomer		2	>9	-	-	-	-
4i		3.5	10.0	6i		n.e.	n.e.
4j		5.5	2.2	-	-	-	-
4k		5.0	4.0	6k		2	>20
4l		3.0	6.8	-	-	-	-
4m		n.e.	n.e.	-	-	-	-
4n		7.0	16.0	6n		2.8	15
4o		3.6	0.2	-	-	-	-
4p		n.e.	n.e.	-	-	-	-
4q		4.0	0.9	6q		2.5	5.0
4r		3.6	3.3	6r		3	10

Table 1. continued

No.	Structure ^a	A _{max} ^b fold	AC ₅₀ ^b μM	No.	Structure ^a	A _{max} ^b fold	AC ₅₀ ^b μM
4s		4.8	2.0	6s		3.4	7
4t		3.0	14.0	-	-	-	-
4u		3.7	0.6	6u		1.5	0.5
4v		3.6	0.7	-	-	-	-
PIFtide	(24mer peptide)	3.4	1.0	-	-	-	-

^aAll compounds were tested as racemates except the **4h** enantiomer and diastomer. ^bMean value of at least two independent experiments, standard deviation <20%. A_{max}: maximum activation of PDK1 compared to DMSO control (=100%); AC₅₀: concentration required for half-maximum activation; n.e.: no effect.

assay conditions than the PIF pocket-binding peptide PIFtide (Table 1).

To gain insight into the binding mode and the essential interactions of the dicarboxylic acid compounds with the protein, we cocrystallized **4h** by soaking the compound with the His-PDK1 50-556 crystal. X-ray analysis revealed that binding solely occurred in the PIF pocket (Figure 2; crystallographic details will be published elsewhere⁴⁴). The overall binding mode was very similar to the one previously published for **II** in complex with PDK1 (PDB code: 3HRF) (see overlay in Figure 2A). Both phenyl rings occupied the two hydrophobic subpockets separated by Leu155, whereby ring B exhibited T-shaped CH- π interactions with Phe157. The protein crystal specifically selected the *S*-enantiomer of **4h**, probably driven by the more favorable carboxylic side chain interactions. One of the two carboxylates occupied a position similar to that found with **II**, interacting with Lys76, Thr148, and Arg131.

The second carboxylate group formed an additional salt bridge with Arg131 as the sole interaction with the binding site (Figure 2B). Obviously, the ionic interaction (distance to Arg131: 3.2 Å) was preferred over the also possible H-bond formation with Gln150 (distance to Gln150-N: 3.5 Å) and was mainly responsible for the increase in potency of the dicarboxylic acid compounds. This observation highlighted again the importance of Arg131 for high binding affinity.

While the X-ray structure substantiated that **4h** exploited most of the molecular interactions achievable for a small molecule with the active conformation of the PIF pocket, it did not provide direct evidence for H-bond formation with the Gln150 and Thr128 side chains. To establish H-bonding with at least one of these residues bordering the PIF pocket is straightforward to further enhance binding affinity without having to increase considerably the molecular mass and was therefore another goal of our compound design. At least it was noticeable that, in spite of the too large distance in the cocrystal (3.6 Å), the ketone of **4h** and the Thr128-OH from helix α -C already appeared appropriately oriented toward each other. It should be considered that the cocrystal structure appears to represent one of the most active states of the kinase⁴⁴ and that H-bond formation between the ketone and Thr128 may be relevant at other conformational states. The same could be true

for the interaction between the carboxylate oxygen and the Gln150 carboxamide group.

Structure-Activity Relationships of the 1,3-Diaryl Malonyl Propanones. Although there was obviously a predominant contribution of the dicarboxyl moiety to the affinity, the activity could be further improved by optimization of the ring substituents. A comparison of the test compounds **4a** and **4b** (Table 1) suggested a somewhat higher potency of the *para*-substituted compound, so we prioritized this position for systematic variation of further substituents. Within the *p*-halogen substituted series, the AC₅₀ improved in the order Cl, Br, I at comparable 4-fold activation efficacies. The iodine analogue **4f** showed a significantly reduced AC₅₀ in the high nanomolar range (0.4 μM). A particular enhancement of potency by iodine was also observed in the homologous set **4c**, **4e**, and **4g**. The increase in affinity according to estimates based on the AC₅₀ values was only 1.8-fold from **4a** (4-Cl) to **4d** (4-Br), but 3.5-fold from **4d** to **4f** (4-I), and 6-fold from **4e** (4-Br) to **4g** (4-I). Altogether, these SARs prompted our speculation that halogen bonding might be involved, which is most strongly mediated by iodine.⁴⁵ It is conceivable that *p*-iodine might take the place of the trifluoromethyl group from **4h** in the hydrophobic subpocket and interact with the Lys115 backbone carbonyl. A similar strong effect of the iodine was observed previously with allosteric inhibitors of PKC ζ that are binding to the homologous PIF pocket.^{46,47}

Looking at the efficacy, we found that, interestingly, the *para*-trifluoromethyl malonic acid derivative **4h** activated PDK1 to a higher degree than PIFtide (5.5-fold vs 3.4-fold activation, respectively, Table 1). The particular effect of the trifluoromethyl substituent might be related to the multiple interactions with the helix α -B area (Figure 2B): the hydrophobic interactions with Val124, Ile 118, and Ile119 are complemented by an orthogonal multipolar interaction with the backbone carbonyl from Lys115. Although the C=O...F distance in the latter case (3.9 Å) is not among the short distance contacts observed in several cocrystal structures (between 2.9 and 3.1 Å), it falls into the more abundant range of observed distances, and the angles between the C-F bond and the carbonyl plane match the average of typical values (C=O...F: 102.5°; C-F...O: 128.3°).⁴⁸ Thus, the orthogonal interaction, albeit weak

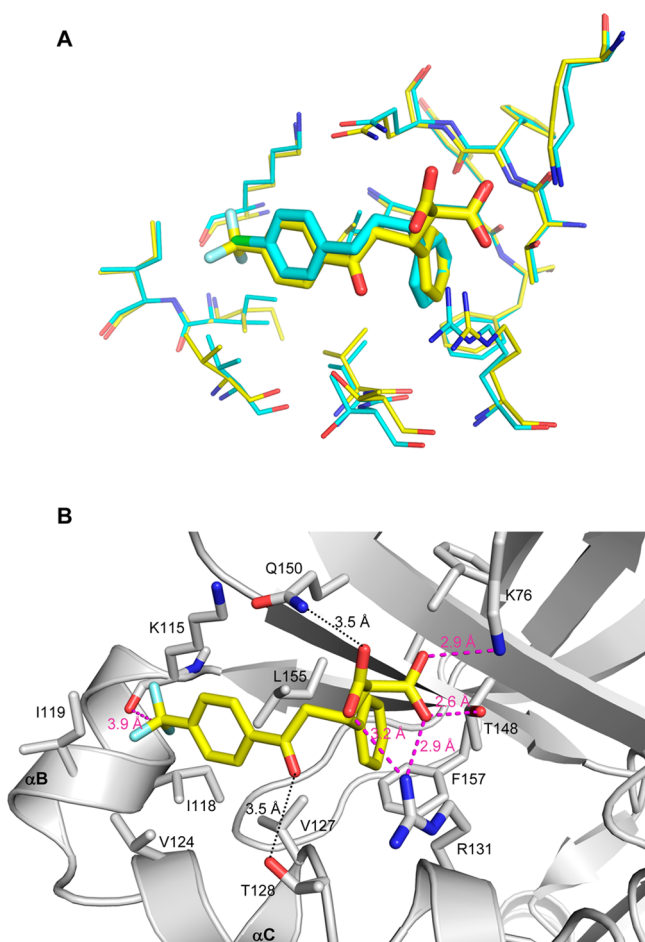


Figure 2. Cocystal structure of compound **4h** complexed with the PIF-pocket of PDK1. (A) Superimposition of the PIF pockets with **4h** (yellow) and **II** (cyan) (PDB code: 3HRF) as bound ligands, respectively. The binding modes of **4h** and **II** present in the cocystal structures are largely identical. The phenyl rings of both compounds bind to the same subpocket areas, and the carboxylate of **II** exactly superimposes with one of the **4h** carboxyl functions, exhibiting the same set of interactions. Arg131 in the **4h** cocystal has moved to establish additional interactions with the second carboxylate. (B) Interactions of **4h** (yellow) with the PIF pocket. Dashed lines in magenta indicate directed polar interactions comprising ionic interactions, H-bonding (with Thr148), and fluoro-carbonyl interaction (Lys115 carbonyl); distances are given in angstrom. Dotted lines with distances indicated in black denote potential additional H-bonding interactions in other conformational states. It is also noteworthy that the depicted Thr128 rotamer with the hydroxyl pointing to the **4h** keto function is not present in the cocystal with **II** (cf. A). Phenyl ring B (see Figure 1) additionally contributes to the binding energy by forming edge-to-face CH- π interactions with Phe157. The image was generated using PyMOL (<http://pymol.sourceforge.net/>).

by itself, might increase the affinity synergistically with the hydrophobic contacts.

In comparison, the 4-ethylphenyl derivative **4k** also exhibited a pronounced activation; however, it was binding with 2-fold lower affinity as assessed from the AC_{50} . Interestingly, the highest possible PDK1 activation was not yet reached by **4h** and **4k**, since **4n** was able to induce a 7-fold increase in PDK1 catalytic activity; however, significantly higher concentrations were needed to achieve this high activation, as reflected by the poor AC_{50} of 7 μM . A similar tendency was observed for the

benzazepin-2-one analogues in the study of Wei et al., where some compounds achieved a more than 10- to 14-fold activation of the PDK1 construct used, which was however accompanied by AC_{50} values estimated to exceed 15 μM .³⁴ However, within a certain range of maximum activation, there was no strict correlation with AC_{50} values both in our present and previous series of PDK1 activators.³¹ For instance, compounds **4g**, **4h**, and **4s** displayed the same AC_{50} values, while their activation efficacies were quite different. Presumably, these compounds bound to and stabilized distinct conformations of the PIF pocket, while the complex formation in each case proceeded with similar affinity constants. A comparison of different PDK1-activator cocystal structures (PDB codes: 3HRF, complex with PS48; 4AW1, complex with **4h**) with the apo form (PDB code: 3HRC) proves that different activators indeed stabilize different conformations that possess distinct catalytic capacities; while the less potent activator PS48 from our previous study (**II** in Figure 1) induced a local movement of the active site Lys111 and ordering of the activation loop,³² only **4h** was able to stabilize a more closed active structure of the catalytic domain of PDK1.⁴⁴ On the other hand, compounds **4a**, **4f**, and **4q** activated PDK1 to the same degree, while their AC_{50} values were quite different. Presumably, these compounds allosterically stabilized PDK1 conformations of similar catalytic activity but exhibited different binding affinities to the corresponding conformations of the PIF pocket.

Since **4h** was endowed with several favorable properties (see also below), the racemic mixture was separated by chiral high-performance liquid chromatography (HPLC) to analyze the biological activity of the individual enantiomers. We noticed that nearly all of the biological activity was confined to one enantiomer, which had been eluted from the column with the higher retention time. Due to limited amounts of material, it was not possible to determine the absolute configuration for the two peak fractions. However, the cocystal structure suggested that the *S*-enantiomer is the eutomer, since it was selected by the crystallized protein from the racemate and presented with a strong electron density, thus ruling out any mixed occupancy of the PIF pocket by both enantiomers. The sharp discrimination can be explained by the interactions visible in the cocystal that make clear that only the *S*-enantiomer of **4h** is able to form two salt bridges with Arg131 (Figure 2).

Additional introduction of a chlorine into phenyl ring B in the 4-position of the above presented compounds **4a**, **4d**, **4f**, **4h**, and **4k** abolished the activating effect on PDK1 considerably. Presumably, this halogen in the *para* position impaired the edge-to-face interaction with Phe157. In contrast, the activity did not decrease when introducing a chlorine atom in the 2-position of phenyl ring B (compound **4j**) suggesting unfilled space around this position that could be exploited to further increase potency by appropriate substituents. The complete lack of activity of **4m** showed that polar functional groups are not well tolerated by the subpocket that accommodates ring A. The 4-phenylthiophene analogue **4p** was synthesized in order to probe whether an elongated aromatic ring system could be forced to enter deeper regions of the pocket, for example, by pushing away the phenyl of Phe157, which apparently did not happen. On the other hand, condensed aromatic ring systems were generally found to be more favorable for affinity, as seen with **4o** (AC_{50} = 0.2 μM , Table 1), and even well tolerated at both ends of the compound as exemplified by **4s**. The positive trend observed for the naphthyl compound **4q** was further corroborated by the

phenanthrene derivative **4u** and the carbazole analogue **4v**, resulting in potent activators with submicromolar AC_{50} values.

The second substance class presented here, the monoacid derivatives (right portion of Table 1), generally exhibited reduced potency compared with the corresponding dicarboxyl analogues, corroborating the importance of the second carboxylate for the enhancement of both affinity and efficacy of activation.

Obviously, the single negative charge of one carboxyl moiety was not sufficient to satisfy the two cationic residues surrounding the PIF pocket, Lys76 and Arg131. Similarly, phosphotyrosine mimetics had also been reported to benefit from two negative charges, for example, provided by a malonic acid residue or by a combination of carboxylate and tetrazole. Cyclohexylmalonic acid was identified as a potent phosphotyrosyl mimetic in a nonpeptidic C-terminal SH2 domain inhibitor of the Syk tyrosine kinase.⁴⁹ In the case of growth factor receptor-bound protein-2, dicarboxyl analogues bound to the SH2 domain with a strength similar to the phosphonate-based phosphotyrosyl mimetics.⁵⁰ However, it remains unclear whether the malonic acid moiety of the 2-(3-oxo-1,3-diphenylpropyl)malonic acids **4a–v** occupies the same position as the phosphate of the natural HM phosphopeptides.

Moreover, the matched pairs of di- and monocarboxylate analogues allowed us to analyze the relative contribution of the second carboxylate in dependence on further variations at the aromatic rings. Notably, fused aromatic rings appeared to increase the CH- π and van der Waals interactions to a level where the overall binding affinity became less dependent on the ionic interactions, as exemplified by **6q**, **6s**, and **6u** compared to their dicarboxylate counterparts **4q**, **4s**, and **4u**. These findings suggested that it might be possible to combine a bicyclic aromatic system, especially a more drug-like benzoheterocycle, as ring B with less acidic moieties, such as sulfonamides, without a substantial loss of potency.

The hydroxynaphthyl derivative **6r** was designed to probe potential H-bond formation with the Lys115 carbonyl (cf. Figure 2B). However, the loss of activity compared to **6q** indicated that this either did not happen or did not provide sufficient energy gain to outbalance the desolvation enthalpy of the polar hydroxyl group in the mostly hydrophobic subpocket.

It should be noted that the AC_{50} values given in Table 1 can only be a rough measure for the relative affinity of the modulators described here. Although we observed a correlation with the K_d values in our previous study, the AC_{50} values of some of the compounds presented herein approached or went below the concentration of PDK1 protein in the assay, which was 0.25 μ M. Thus, a linear relationship between AC_{50} and K_d could not be expected. Our attempts to accurately measure K_d values using isothermal calorimetry were hampered by the strongly exothermic dilution reaction of the dicarboxylic acid compounds that conferred a high error rate to the much lower binding enthalpy. As an alternative to compare the binding affinity of our small molecule ligands with that of PIFtide, we analyzed the compound-mediated thermal stabilization of PDK1 using differential scanning fluorimetry (DSF). It was previously shown that the potency of a kinase inhibitor to increase the denaturation temperature of the protein structure was proportional to its binding affinity, both in the case of ATP-competitive⁵¹ and non-ATP-competitive compounds.⁵² Analyzing the effect of our most potent modulators ($AC_{50} < 1 \mu$ M) along with PIFtide on the thermal stabilization of PDK1, we found that the EC_{50} values of **4o** and **4v** were comparable

that of the 24-mer peptide PIFtide (13.0 and 30.2 μ M vs 14.2 μ M, respectively, Table 2). However, PIFtide raised the

Table 2. Potencies of Compounds 4f, 4h, 4o, and 4v to Increase the Thermal Stability of PDK1 in Comparison to PIFtide^a

compd no.	EC_{50} (μ M)	ΔT_m max ^b ($^{\circ}$ C)	$c(\Delta T_m 1.5^{\circ}$ C) ^c (μ M)
4f	60.0	5.2	30.9
4h	85.8	3.9	67.6
4o	13.0	2.4	18.9
4v	30.2	4.9	18.2
PIFtide	14.2	7.3	3.1

^aValues from one of two independent experiments are shown that gave essentially similar results. The standard deviation was <15% for all ΔT_m values used to calculate the EC_{50} . ^bMaximum shift of thermal stability. ^cConcentration required to increase thermal stability by 1.5 $^{\circ}$ C.

denaturation temperature to a higher level than any of the small molecules ($\Delta T_m = 7.3^{\circ}$ C, Table 2), suggesting that potencies should not be compared solely based on the EC_{50} values. Therefore, the concentration required to produce a ΔT_m shift of 1.5 $^{\circ}$ C was calculated as a further parameter. This ΔT_m was chosen because it was located in the linear slope of the sigmoidal EC_{50} curve for each compound. Again, **4o** and **4v** emerged as the most potent small ligands, both requiring 6-fold higher concentrations than PIFtide to increase the ΔT_m by 1.5 $^{\circ}$ C. Taken together, the potencies of our best modulators, **4o** and **4v**, and PIFtide to enhance the thermal stability to PDK1 were in the same order of magnitude. This suggested that the affinities to the PIF pocket were also comparable, especially since the high binding affinity of PIFtide is only reached by interacting with additional sites outside the PIF pocket. Thus, it is reasonable to assume that the small molecule ligands are able to effectively compete with PIFtide and HM peptides with lower affinity by blocking the “hot spot” PIF pocket. Compound **4h** was included in the thermal stability shift assay to assess whether the AC_{50} values might correlate with the potency to protect against denaturation. Indeed, **4h** was found to be the weakest stabilizer of PDK1, in agreement with the significantly higher AC_{50} value of **4h** compared to the other three compounds.

1,3-Diaryl Malonyl Propanones Are Highly Selective for PDK1. The selectivities of the 2-(3-oxo-1,3-diphenylpropyl)-malonic acids were evaluated toward a panel of AGC kinases, which all share a homologous PIF pocket with PDK1. If at all, there was only a weak influence on the other AGC kinases examined. Some selectivity data is exemplarily given for **4a** and **4h** in Table 3. Only at concentrations of about 25-times the AC_{50} value for PDK1, **4a** and **4h** appeared to inhibit S6K by about 50% and had a marginal activating effect on RSK. These results demonstrate that, despite the similarity of the homologous PIF pockets, differences suffice to develop highly selective modulators.

Since kinases not belonging to the AGC family do not possess an equivalent binding pocket, it was expected that these should not be affected by the allosteric modulators. Indeed, compound **4h** did not show any effect on 121 further kinases representing all branches of the kinome in our parallel study.⁴⁴

Cell Permeation Studies Involving a Prodrug Strategy. All dicarboxylic acid compounds were inactive in cellular assays due to the high polarity of the carboxylate groups. In a first

Table 3. Selectivity Profile of Compound II and the Dicarboxyl Compounds 4a and 4h^a

compd no.	μM	PDK1	S6K1	PKC ζ	SGK	PKB α	PKA	PRK2	RSK	MSK
II	2	n.e.	n.e.	n.e.	n.e.	n.e.	n.e.	n.e.	n.d.	n.d.
	50	242	84	n.e.	n.e.	n.e.	74	n.e.	n.d.	n.d.
4a	2	228	84	n.e.	n.e.	n.e.	n.e.	n.e.	n.e.	n.e.
	50	558	47	n.e.	n.e.	n.e.	n.e.	n.e.	160	n.e.
4h	2	305	82	n.e.	n.e.	n.e.	n.e.	n.e.	n.e.	n.e.
	50	637	46	n.e.	n.e.	n.e.	80	n.e.	140	n.e.

^aValues show the % catalytic activity of the DMSO-treated control (= 100%); n.e.: no effect; n.d.: not determined. Each value is representative of at least two independent assays that essentially gave the same results.

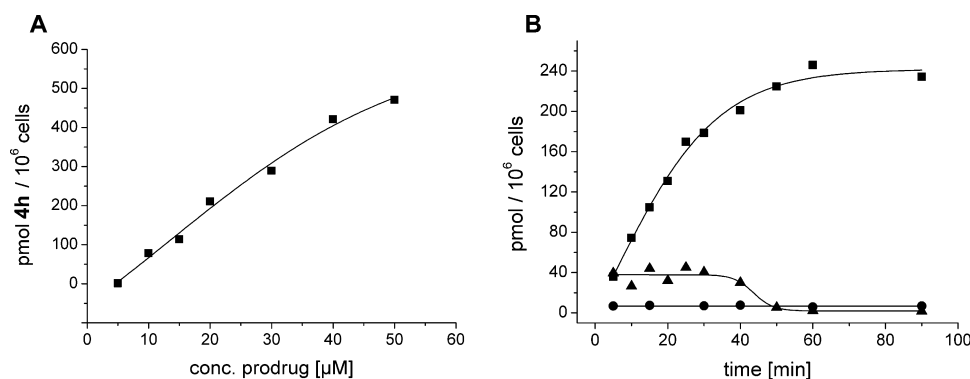


Figure 3. Prodrug **5h** is efficiently taken up by rat L6 cells and converted into the active compound **4h**. (A) Dependency of intracellular formation of **4h** on the prodrug concentration. L6 cells were incubated for 2 h with the indicated concentrations of the prodrug **5h** and then extracted with ethylacetate, and the content of **4h** was quantified using HPLC-MS/MS. (B) Time course of the intracellular accumulation of **4h** and concomitant disappearance of the prodrug **5h**. L6 cells were incubated with 20 μM of the prodrug **5h** or of **4h** for the indicated times, the cells were extracted, and the compounds were quantified. Analysis revealed that **4h** (■) is released from **5h** (◆) in a time-dependent manner, whereas **4h** itself is not cell-permeable (●).

attempt to achieve cellular delivery, we utilized the corresponding methyl and ethyl esters of the 2-(3-oxo-1,3-diphenyl-propyl)malonic acids that were readily available as synthetic precursors. However, these derivatives displayed no cellular activity either, suggesting that they were resistant to hydrolysis by esterases. Hence, we decided to synthesize esters with higher enzymatic lability; in this regard, acyloxyalkyl esters represent established prodrug moieties that are in therapeutic use; for instance, the penicillin derivative pivampicillin exhibits improved bioavailability, whereas simple alkyl esters of penicillin lacked therapeutic potential.^{53–56}

We synthesized the bisacetoxymethyl esters **5a**, **5h**, and **5q** starting from the corresponding malonic acid derivatives **4a**, **4h**, and **4q** (Scheme 1). In the cell-free assay, these ester derivatives were completely inactive like all simple alkyl esters that we tested. However, the *para*-trifluoromethyl-phenyl prodrug analogue **5h** showed the most promising activity in a preliminary cellular screening, so we selected this compound for a detailed analysis of the concentration and time dependency of prodrug cleavage to identify optimal conditions for cell assays. Initially, we checked the chemical stability of the ester prodrug **5h** in cell-free medium at 37 °C; under these conditions, the half-life due to spontaneous hydrolysis was 4.8 h, suggesting that no significant degradation would occur in the absence of esterases outside the cells.

To evaluate the cellular conversion of the prodrug, the rat L6 skeletal muscle cell line was chosen as a model because it derives from a potential target tissue for antidiabetic drugs and displays acetoxymethyl esterase activity in the postfusional form.⁵⁷ The intracellular accumulation of the ester prodrug **5h** and the corresponding malonic acid derivative **4h** was

monitored by mass spectrometry (MS) after extraction of the compounds under acidic conditions using ethyl acetate.

First, we aimed to analyze the concentration dependency of the prodrug conversion to the free malonic acid derivative in the cells. As can be seen from Figure 3A, the rate of conversion showed little concentration dependency over a wide range. Only at concentrations higher than 40 μM , saturation of the intracellular enzyme began to show. For the subsequent experiment, we chose a prodrug concentration of 20 μM .

The bisacetoxymethyl ester **5h** exhibited a high membrane permeation rate as judged from its appearance inside the cells already after 5 min (Figure 3B). However, it reached only moderate concentrations and declined steadily thereafter, most likely because of the rapid conversion to the free dicarboxylic acid analogue **4h** in the cytoplasm. Based on the measured rate of **4h** production, the rate constant of hydrolysis in the cells was calculated to be 67 times higher than that of the uncatalyzed reaction, reducing the half-life of **5h** to 4.3 min.

The dicarboxylate compound **4h** concomitantly accumulated in the cells until it reached a plateau after approximately 1 h. The main reason for this halt of increase was the depletion of the prodrug compound from the medium. In a further experiment, we observed that, after one hour, the prodrug form was degraded to more than 90% in the cell medium. Since this was considerably faster than the spontaneous hydrolysis, the degradation was probably caused by esterases leaking from the cells. The maximum levels of **4h** reached in the cells can roughly be estimated to be 80 μM , if an average cell volume of 3 pL is assumed.^{58,59} This suggested that the dicarboxylic acid compound became trapped and was about 4-fold enriched in the cells.

In sharp contrast to the prodrug, the free malonic acid analogue could not be detected, neither in the soluble nor in the insoluble cell fractions under the same incubation conditions (closed circles in Figure 3B, and data not shown). Having established that **4h** was released from its prodrug form, we analyzed the gross intracellular distribution of **4h** in a further experiment. To this end, treated cells were disrupted by sonication and centrifuged at high speed. Subsequent HPLC-MS analysis showed that the product **4h** of the enzymatic conversion was only detectable in the soluble fraction, excluding accumulation in the membrane (data not shown).

Effects of the Prodrug 5h on the Phosphorylation of S6K, PKC ζ , and PKB in Intact Cells. The effects of **5h** on PDK1-catalyzed phosphorylations were investigated in HEK293 cells. To analyze the influence on the phosphorylation state of the activation loops of S6K and PKC ζ , the cells were transfected with expression plasmids encoding GST-S6K[T412E] and GST-PKC ζ , and the recombinant proteins were isolated after cell treatment with **5h** or DMSO and stimulation by insulin-like growth factor (IGF)-I. Probing of the western blots with phospho-specific antibodies revealed that **5h** decreased the phosphorylation of the S6K activation loop, while there was no significant effect on the PKC ζ Thr410 phosphorylation (Figure 4A). This result indicated that **4h**, which was generated in the

cells, bound to the PIF pocket, thereby preventing phosphorylation of S6K at the activation loop residue Thr229. In contrast, transient blockage of the PDK1 PIF pocket did not significantly affect the activation loop phosphorylation of PKC ζ , confirming the hypothesis that PKC is constitutively phosphorylated by PDK1. Only permanent blockage of the PIF pocket, for example, as exerted by cellular overexpression of GST-PIFtide in the study of Balendran et al.,²⁸ would probably prevent activation loop phosphorylation of newly synthesized PKC ζ . In another experiment, nontransfected HEK293 cells were identically treated with the prodrug **5h** or a DMSO control followed by IGF-I stimulation, and the cell lysates were directly used for immunoblotting. The antibodies used here did not require prior overexpression or pull-down of the proteins. Upon treatment with **5h**, phosphorylation of the ribosomal S6 protein by S6K was strongly inhibited (Figure 4B), indicating that the reduction of the activation loop phosphorylation by PDK1 resulted in a diminished catalytic activity of S6K. Importantly, treatment of the HEK293 cells with **5h** did not significantly inhibit the PDK1-dependent T-loop phosphorylation of PKB, which is in line with similar experiments performed by us using C2C12 myoblasts.⁴⁴

CONCLUSIONS

The introduction of a second negatively charged carboxylate resulted in a strong increase of potency of the new PDK1 modulator class presented in this study, yielding several compounds that allosterically activated PDK1 at submicromolar concentrations. According to our thermal stability shift assay results, some of the 2-(3-oxo-1,3-diphenylpropyl)malonic acids are expected to possess binding affinities to the PIF pocket in a range comparable to that of PIFtide. Thus, further considering that the PIF pocket might truly represent a "hot spot" due to its interaction with the core motif of the HM peptide, the allosteric ligands should be able to effectively compete with substrate HM peptides for the binding to the PIF pocket in cells. Indeed, our results indicated that blockage of the pocket is the major cellular effect of the compounds binding to the PIF pocket, which is independent of whether the compound is an activator of PDK1 in the cell-free assay. The remarkable selectivity of the compounds for PDK1 confirmed once again that, by targeting less conserved allosteric sites, modulators even specific for a single kinase might be developed.

To enable the cellular delivery of the highly polar compounds, we applied an established prodrug strategy. The prodrug **5h** efficiently reached the cytoplasm and was readily converted to the active malonic acid derivative **4h**. Altogether, we developed a new series of PIF pocket ligands that are potent and selective enough to conduct the first detailed validation studies in cells. The pharmacological profile of allosteric PIF pocket ligands is expected to be novel and distinct from type I and type II inhibitors directed to the ATP-binding site. In first experiments, we analyzed the effects of our prodrug **5h** on key substrates of PDK1 that play major roles in insulin-dependent signaling, namely, S6K, PKC ζ , and PKB. The following short-term cellular effects of **5h** were observed: inhibition of S6K phosphorylation and activation with no influence on PKC ζ and PKB. Hence, further studies will be designed to evaluate whether targeting the PIF pocket could become a novel approach for the treatment of diabetes type 2.

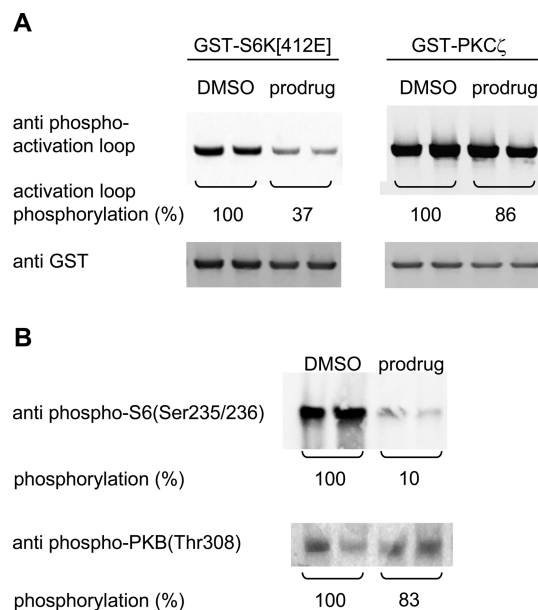


Figure 4. Effect of the prodrug **5h** on the PDK1 substrates S6K, PKC ζ , and PKB in intact cells. (A) HEK 293 cells were transfected with GST-S6K[412E] and GST-PKC ζ , incubated with 50 μ M **5h** for 2 h, and stimulated by IGF-I for 20 min. The recombinant proteins were isolated and analyzed by immunoblotting using antibodies detecting the activation loop phosphorylations. Signals from the same blots probed with anti-GST antibody were used to normalize the quantified phosphorylation levels. (B) Serum-starved HEK293 cells were treated with 50 μ M **5h** for 2 h and stimulated by IGF-I for 20 min. Cell lysates were analyzed by immunoblotting using phospho-specific antibodies as indicated. Antiphospho-S6(Ser235/236) detects S6K-dependent phosphorylations in the ribosomal S6 protein, and Thr308 is the PDK1 phosphorylation site in the activation loop of PKB. Normalization of the quantified phosphorylation signals was done after reprobing the blots with antiactin antibody (not shown). In (A) and (B), one representative experiment out of two separate experiments is depicted.

EXPERIMENTAL SECTION

Chemical Methods. Solvents and reagents were obtained from commercial suppliers and were used without further purification. Flash column chromatography was carried out using silica-gel 40 (35/40–63/70 μM) with hexane/ethyl acetate mixtures as eluents, and the reaction progress was determined by thin-layer chromatography (TLC) analysis on Alugram SIL G/UV₂₅₄ (Macherey–Nagel). Visualization was accomplished with UV light. ^1H NMR and ^{13}C spectra were recorded at 500 MHz on a Bruker DRX-500 spectrometer. ^1H shifts are referenced to the residual protonated solvent signal (δ 2.50 for DMSO- d_6 and δ 7.26 for CDCl_3), and ^{13}C shifts are referenced to the deuterated solvent signal (δ 39.5 for DMSO- d_6 and δ 77.2 for CDCl_3). Chemical shifts are given in parts per million (ppm), and all coupling constants (J) are given in hertz. The purities of the title compounds **4a–v**, **5a**, **5h**, **5q**, **6a–d**, **6f–i**, **6k**, **6n**, **6q–s**, and **6u** were determined by HPLC coupled with mass spectrometry and were higher than 95% in all cases.

Mass spectrometric analysis (HPLC-ESI-MS) was performed on a TSQ quantum (Thermo Electron Corporation) instrument equipped with an electrospray ionization (ESI) source and a triple quadrupole mass detector (Thermo Finnigan, San Jose, CA). The MS detection was carried out at a spray voltage of 4.2 kV, a nitrogen sheath gas pressure of 4.0×10^5 Pa, an auxiliary gas pressure of 1.0×10^5 Pa, a capillary temperature of 400 °C, a capillary voltage of 35 V, and source CID of 10 V. All samples were injected by autosampler (Surveyor, Thermo Finnigan) with an injection volume of 10 μL . A RP C18 NUCLEODUR 100-3 (125 mm \times 3 mm) column (Macherey–Nagel) was used as the stationary phase. The solvent system consisted of water containing 0.1% TFA (A) and 0.1% TFA in acetonitrile (B). HPLC method was as follows: the flow rate was 400 $\mu\text{L}/\text{min}$. The percentage of B started at an initial 5%, was increased to 100% during 16 min, kept at 100% for 2 min, and flushed back to 5% within 2 min. All masses were reported as protonated parent ions. Melting points (mp) were determined in open capillaries on a Mettler FP1 melting point apparatus and are uncorrected.

General Synthetic Methods and Experimental Details for Some Key Compounds. *Method A: Claisen–Schmidt Condensation, for the Preparation of 1a–v.* The corresponding benzaldehyde (1 equiv) was dissolved in EtOH (2 mL per mmol of aldehyde), 3 M NaOH_{aq} solution (1 mL per mmol of aldehyde) and acetophenone (1 equiv) were added, and the resulting mixture was stirred at rt for 2 h forming a yellow precipitate. The yellow solid was separated by vacuum filtration and was washed three times with 10 mL of ice water. The crude product was purified by recrystallization from MeOH.

(E)-3-Phenyl-1-(4-(trifluoromethyl)phenyl)prop-2-en-1-one (1h). Synthesized according to method A using benzaldehyde (1.62 mL, 15.95 mmol) and 1-(4-(trifluoromethyl)phenyl)ethanone (3.0 g, 15.95 mmol); pale yellow solid; yield: 3.05 g (70%); ^1H NMR (500 MHz, CDCl_3): δ (ppm) = 7.49–7.43 (m, 3H), 7.50 (d, J = 15.8 Hz, 1H), 7.67–7.65 (m, 2H), 7.77 (d, J = 8.0 Hz, 2H), 7.84 (d, J = 15.8 Hz, 1H), 8.10 (d, J = 8.0 Hz, 2H); ^{13}C NMR (125 MHz, CDCl_3): δ (ppm) = 121.6, 123.6 (q, $^1J_{\text{C-F}}$ = 272.9 Hz), 125.69 (q, $^3J_{\text{C-F}}$ = 4.3 Hz), 128.6, 128.8, 129.0, 130.9, 133.9 (q, $^2J_{\text{C-F}}$ = 32.3 Hz), 134.5, 141.1, 146.1, 189.7.

(E)-1-(4-Iodophenyl)-3-(naphthalen-2-yl)prop-2-en-1-one (1o). Synthesized according to method A using 2-naphthaldehyde (1.90 g, 12.19 mmol) and 4'-iodoacetophenone (3.0 g, 12.19 mmol); pale yellow solid; yield: 3.90 g (83%); ^1H NMR (500 MHz, CDCl_3): δ (ppm) = 7.51–7.56 (m, 2H), 7.58 (d, J = 15.6 Hz, 1H), 7.76 (d, J = 8.5 Hz, 2H), 7.76–7.80 (m, 1H), 7.82–7.89 (m, 3H), 7.88 (d, J = 8.5 Hz, 2H), 7.98 (d, J = 15.6 Hz, 1H), 8.04 (s, 1H); ^{13}C NMR (125 MHz, CDCl_3): δ (ppm) = 100.6, 121.6, 123.6, 126.8, 127.5, 127.8, 128.7, 128.8, 129.9, 130.8, 132.2, 133.4, 134.5, 137.6, 137.9, 145.5, 189.6.

Method B1: Michael Addition Reaction, for the Preparation of 2a, 2b, 2d, 2h, 2k, 2n, 2p–s, and 2u–v. The corresponding chalcone (1 equiv) and magnesium oxide (0.1 g per 0.1 mmol of chalcone) were dissolved in toluene, and diethyl malonate (1 equiv) was added. The reaction was stirred at rt for 2 h. The magnesium oxide was separated by vacuum filtration and was washed three times with 10

mL of dichloromethane. The solvent was evaporated, and the crude product was crystallized from diethyl ether and hexane.

Diethyl 2-(3-Oxo-1-phenyl-3-(4-(trifluoromethyl)phenyl)propyl)malonate (2h). Synthesized according to method B1 using (*E*)-3-phenyl-1-(4-(trifluoromethyl)phenyl)prop-2-en-1-one (1.5 g, 5.42 mmol) and diethyl malonate (0.82 mL, 5.92 mmol) and magnesium oxide (0.54 g); white solid; yield: 1.8 g (76%); ^1H NMR (500 MHz, $(\text{CD}_3)_2\text{SO}$): δ (ppm) = 0.85 (t, J = 7.2 Hz, 3H), 1.16 (t, J = 7.2 Hz, 3H), 3.46 (dd, J = 3.8, 17.0 Hz, 1H), 3.69 (dd, J = 3.8, 17.0 Hz, 1H), 3.83 (q, J = 7.2 Hz, 2H), 3.90–3.98 (m, 2H), 4.08–4.18 (m, 2H), 7.15 (t, J = 7.6 Hz, 1H), 7.22 (d, J = 7.6 Hz, 2H), 7.29 (d, J = 7.8 Hz, 2H), 7.87 (d, J = 8.2 Hz, 2H), 8.05 (d, J = 8.2 Hz, 2H); ^{13}C NMR (125 MHz, $(\text{CD}_3)_2\text{SO}$): δ (ppm) = 13.4, 13.7, 40.4, 56.7, 60.6, 61.2, 116.2, 116.4, 125.6 (q, $^3J_{\text{C-F}}$ = 3.7 Hz), 126.8, 127.9, 128.2, 128.5, 140.2, 167.7, 168.4, 197.2.

Method B2: Michael Addition Reaction, for the Preparation of Diethyl 2-(1-(4-Chlorophenyl)-3-(4-iodophenyl)-3-oxopropyl)malonate (2g). (*E*)-3-(4-chlorophenyl)-1-(4-iodophenyl)prop-2-en-1-one (2.0 g, 4.07 mmol) and diethyl malonate (0.68 mL, 4.47 mmol, 1.1 equiv) were dissolved in ethanol, and potassium carbonate (1.12 g, 8.14 mmol, 2 equiv) was added. The mixture was heated at reflux for 2 h. The reaction was quenched with H_2O (50 mL) and extracted with CH_2Cl_2 (3 \times 20 mL). The organic layer was washed with brine, dried with MgSO_4 , and evaporated under vacuum. The crude product was crystallized from methylene chloride and hexane; pale beige solid; yield: 0.86 g (40%); ^1H NMR (500 MHz, CDCl_3): δ (ppm) = 1.05 (t, J = 7.2 Hz, 3H), 1.25 (t, J = 7.2 Hz, 3H), 3.35 (dd, J = 9.5, 9.5 Hz, 1H), 3.49 (dd, J = 4.1, 4.1 Hz, 1H), 3.76 (d, J = 9.8 Hz, 1H), 3.98 (q, J = 7.2 Hz, 2H), 4.09–4.25 (m, 3H), 7.18 (d, J = 8.8 Hz, 2H), 7.22 (d, J = 8.8 Hz, 2H), 7.59 (d, J = 8.8 Hz, 2H), 7.79 (d, J = 8.8 Hz, 2H); ^{13}C NMR (125 MHz, CDCl_3): δ (ppm) = 13.8, 14.0, 40.1, 42.3, 57.2, 61.5, 61.8, 101.2, 128.6, 129.5, 129.6, 133.0, 133.9, 138.0, 138.8, 167.5, 168.1, 196.6.

Method B3: Michael Addition Reaction, for the Preparation of 2c, 2e, 2f, 2i, 2j, 2l, 2m, 2o, 2t. The corresponding chalcone (1 equiv) and diethyl malonate (1 equiv) were dissolved in methanol, and sodium hydride (cat.) was added. The mixture was heated at reflux for 2 h. The reaction was quenched with H_2O (50 mL) and extracted with CH_2Cl_2 (3 \times 20 mL). The organic layer was washed with brine, dried with MgSO_4 , and evaporated under vacuum. The crude product was crystallized from methylene chloride and hexane.

Dimethyl 2-(3-(4-Iodophenyl)-1-(naphthalen-2-yl)-3-oxopropyl)malonate (2o). Synthesized according to method B3 using (*E*)-1-(4-iodophenyl)-3-(naphthalen-2-yl)prop-2-en-1-one (1.5 g, 3.90 mmol), diethyl malonate (0.59 mL, 3.90 mmol), and sodium hydride (cat.); pale yellow solid; yield: 1.10 g (55%); ^1H NMR (500 MHz, CDCl_3): δ (ppm) = 3.47 (s, 3H), 3.53 (dd, J = 8.8, 16.9 Hz, 1H), 3.59 (dd, J = 4.7, 16.9 Hz, 1H), 3.73 (s, 3H), 3.95 (d, J = 9.1 Hz, 1H), 4.31–4.36 (m, 1H), 7.39 (dd, J = 1.9, 8.5 Hz, 1H), 7.41–7.45 (m, 2H), 7.60 (d, J = 8.5 Hz, 2H), 7.67 (ds, J = 1.26 Hz, 1H), 7.74–7.77 (m, 3H), 7.78 (d, J = 8.5 Hz, 2H); ^{13}C NMR (125 MHz, CDCl_3): δ (ppm) = 40.8, 42.2, 52.4, 52.7, 57.2, 101.1, 125.9, 126.0, 126.1, 127.6, 127.8, 128.3, 129.5, 132.6, 133.3, 136.0, 137.8, 137.9, 168.0, 168.7, 196.5.

Method C: Hydrolysis, for the Preparation of 4a–v. A solution of the corresponding malonic ester (**2a–l**, **2n–v**, and **3m**) (1 equiv) and 10 M NaOH_{aq} (1–3 mL per mmol malonic ester, as indicated) in EtOH was refluxed for 4 h. After completion of the reaction, the cooled mixture was poured into water (30 mL), acidified to pH 2 with 10% HCl, and extracted with ethyl acetate (3 \times 20 mL). The ethyl acetate extracts were collected and further extracted with aqueous sodium bicarbonate solution (4 \times 20 mL). The pH of the bicarbonate extractions was adjusted to 2 with 10% HCl. White solids formed that were further extracted with ethyl acetate (3 \times 50 mL). The organic solution was dried over MgSO_4 and evaporated to afford a residue consisting of the free acid, which was purified by crystallization.

2-(3-Oxo-1-phenyl-3-(4-(trifluoromethyl)phenyl)propyl)malonic acid (4h). Synthesized according to method C using diethyl 2-(3-oxo-1-phenyl-3-(4-(trifluoromethyl)phenyl)propyl)malonate (1.76 g, 4.03 mmol) and 10 M NaOH_{aq} (6.71 mL); white solid; yield: 1.25 g (82%); mp 128–130 °C; ^1H NMR (500 MHz, CD_3OD): δ (ppm) = 3.53 (d, J

= 9.7 Hz, 1H), 3.56 (d, $J = 6.9$ Hz, 1H), 3.83 (d, $J = 10.9$ Hz, 1H), 4.02–4.08 (m, 1H), 7.14 (t, $J = 7.2$ Hz, 1H), 7.21 (t, $J = 7.6$ Hz, 2H), 7.27 (d, $J = 7.9$ Hz, 2H), 7.75 (d, $J = 8.2$ Hz, 2H), 8.05 (d, $J = 8.2$ Hz, 2H); ^{13}C NMR (125 MHz, CD_3OD): δ (ppm) = 42.6, 44.3, 58.7, 125.2 (q, $^1J_{\text{C-F}} = 272.2$ Hz), 126.7 (q, $^3J_{\text{C-F}} = 3.7$ Hz), 128.0, 129.3, 129.6, 129.8, 135.2 (d, $^2J_{\text{C-F}} = 32.9$ Hz), 141.3, 142.0 (d, $^4J_{\text{C-F}} = 1.8$ Hz), 171.5, 171.8, 199.2; LC/MS (+ESI): $m/z = 381.2$ [MH^+]; $R_t = 4.35$ ($\geq 96\%$).

2-(3-(4-Iodophenyl)-1-(naphthalen-2-yl)-3-oxopropyl)malonic acid (4o). Synthesized according to method C using dimethyl 2-(3-(4-iodophenyl)-1-(naphthalen-2-yl)-3-oxopropyl)malonate (0.7 g, 1.36 mmol) and 10 M NaOH_{aq} (4.4 mL); white solid; yield: 0.5 g (75%); mp 150–151 °C; ^1H NMR (500 MHz, $(\text{CD}_3)_2\text{SO}$): δ (ppm) = 3.41 (dd, $J = 3.5, 17.02$ Hz, 1H), 3.71 (dd, $J = 10.4$ Hz, 1H), 3.85 (d, $J = 10.7$ Hz, 1H), 4.02 (dt, $J = 3.8, 10.4$ Hz, 1H), 7.41–7.46 (m, 2H), 7.50 (dd, $J = 1.6, 8.5$ Hz, 1H), 7.74–7.77 (m, 2H), 7.79–7.82 (m, 2H), 7.86 (d, $J = 8.5$ Hz, 2H), 12.84 (s, 2OH); ^{13}C NMR (125 MHz, $(\text{CD}_3)_2\text{SO}$): δ (ppm) = 40.2, 40.5, 57.3, 101.7, 125.5, 125.8, 126.7, 126.9, 127.2, 127.3, 127.4, 129.5, 131.8, 132.6, 134.4, 135.7, 137.5, 138.7, 168.9, 169.6, 192.4; LC/MS (+ESI): $m/z = 489.2$ [MH^+]; $R_t = 5.05$ ($\geq 97\%$).

Method D: Esterification, for the Preparation of 5a, 5h, and 5q.

To a stirred solution of the corresponding malonic acid derivative or (1 equiv) and NET_3 (5 equiv) in anhydrous DMF (5 mL), bromomethyl acetate (3 equiv) was added. After stirring for 4 h at rt, the mixture was hydrolyzed, extracted with ethyl acetate (3 x), washed with brine, dried over MgSO_4 , filtered, and concentrated at reduced pressure. The residue was purified by flash column chromatography.

Bis(acetoxymethyl) 2-(3-Oxo-1-phenyl-3-(4 (trifluoromethyl)phenyl)propyl)malonate (5h). Synthesized according to method D using 2-(3-oxo-1-phenyl-3-(4-(trifluoromethyl)phenyl)propyl)malonic acid (4h) (0.2 g, 0.52 mmol), bromo methylacetate (0.206 mL, 2.10 mmol), and triethylamine (0.44 mL, 3.12 mmol); white solid; yield: 0.17 g (62%); mp 89–90 °C; ^1H NMR (500 MHz, CD_3OD): δ (ppm) = 1.98 (s, 3H), 2.09 (s, 3H), 3.50 (dd, $J = 8.8$ Hz, 1H), 3.60 (dd, $J = 4.2$ Hz, 1H), 3.96 (d, $J = 9.1$ Hz, 1H), 4.17–4.21 (m, 1H), 5.55 (q, $J = 5.7$ Hz, 2H), 5.76 (d, $J = 5.7$ Hz, 2H), 7.18–7.21 (m, 1H), 7.23–7.28 (m, 4H), 7.69 (d, $J = 8.2$ Hz, 2H), 7.98; ^{13}C NMR (125 MHz, CD_3OD): δ (ppm) = 20.5, 20.6, 40.4, 40.5, 56.5, 79.4, 79.8, 118.0, 125.6 (q, $^3J_{\text{C-F}} = 4.6$ Hz), 127.6, 128.1, 128.4, 128.7, 164.9, 165.8, 166.0, 166.5, 169.2, 169.3, 196.4; LC/MS (+ESI): $m/z = 525.3$ [MH^+]; $R_t = 5.31$ ($\geq 99\%$).

Method E: Decarboxylation, for the Preparation of 6a–d, 6f–i, 6k, 6n, 6q, 6s, and 6u. The corresponding malonic acid derivative (1 equiv) was subject to pyrolytic treatment in an oil bath at 160 °C for 1 h. Heating was stopped after the CO_2 evolution ceased. The crude product was dissolved in acetone/methanol and precipitated with dichloromethane to afford the acid.

5-Oxo-3-phenyl-5-(4-(trifluoromethyl)phenyl)pentanoic acid (6h). Synthesized according to method E using 2-(3-oxo-1-phenyl-3-(4-(trifluoromethyl)phenyl)propyl)malonic acid (4h) (0.10 g, 0.26 mmol); white solid; yield: 0.70 g (68%); mp 99–101 °C; ^1H NMR (500 MHz, CDCl_3): δ (ppm) = 2.75 (dd, $J = 7.0, 16.1$ Hz, 1H), 2.87 (dd, $J = 7.0, 16.1$ Hz, 1H), 3.36 (dd, $J = 6.8, 17.0$ Hz, 1H), 3.42 (dd, $J = 6.8, 17.0$ Hz, 1H), 3.83–3.89 (m, 1H), 7.20 (tt, $J = 1.6, 6.9$ Hz, 1H), 7.22–7.31 (m, 4H), 7.69 (d, $J = 8.2$ Hz, 2H), 7.90 (d, $J = 8.2$ Hz, 2H); ^{13}C NMR (125 MHz, CDCl_3): δ (ppm) = 37.2, 39.9, 44.8, 114.8, 115.3, 116.0, 116.5, 125.7 (q, $^3J_{\text{C-F}} = 3.7$ Hz), 127.1, 127.3, 128.4, 128.8, 175.6, 199.4; LC/MS (+ESI): $m/z = 337.2$ [MH^+]; $R_t = 4.80$ ($\geq 99\%$).

Biological Assays. PDK1 Activity Assay. Determination of the PDK1 activity was performed exactly as described previously.³⁰ In brief, T308tide (KTFCGTPEYLAEVRR) was used as the substrate peptide and the phosphorylation was started by addition of $\gamma\text{-}^{32}\text{P}$ -ATP/ Mg^{2+} . The phosphorylated peptides were captured on P81 phosphocellulose paper (Whatman) and detected by phosphorimaging. The sequence of the reference effector peptide PIFtide was REPRILSEEEQEMFRDFDIADWC.

HPLC-MS/MS Detection of Hydrolysis of the Prodrugs in L6 Cells.

L6 cells were seeded in 10 cm Petri dishes at a density of 10^6 /mL in Dulbecco's modified Eagle's medium (DMEM), supplemented with penicillin/streptomycin and 10% fetal bovine serum (FBS). After having reached confluency, the L6 cells were washed with phosphate-buffered saline (PBS), the medium was replaced by DMEM without FBS, and the cells were treated with the compounds for appropriate time intervals (5–90 min). At the end of the incubation periods, the supernatant was removed, and the cells were washed three times with cold PBS. The cells were harvested by trypsin/EDTA treatment, the cell suspensions were transferred to a flask, and the cells per volume were counted using a Neubauer chamber. At that point, carbamazepine was added to the suspension as an internal standard to determine the recovery rate. One mL of 0.6 N HCl in water was added, and the dicarboxylic acids were extracted using 3 mL of ethyl acetate with shaking of the samples for 20 min. The samples were centrifuged, and 1 mL aliquots of the ethyl acetate supernatants were taken and evaporated to dryness. The samples were resuspended in 500 μL of methanol and used directly for mass spectrometric analysis (HPLC-ESI-MS/MS). The amounts of the compounds were calculated using a standard calibration curve. DMSO-treated cells were processed in parallel and analyzed as a control. The disappearance of the ester and the appearance of the corresponding dicarboxylic acid were additionally confirmed by UV peak quantifications and spiking of the samples with the purified compounds. In the HPLC runs, mobile phase A was water containing 0.5% trifluoroacetic acid, and mobile phase B was methanol containing 0.5% trifluoroacetic acid. From 0 to 8 min, a gradient of 70–100% B was applied, followed by 100% B until the end; sample volume was 25 μL , the flow rate was 0.5 mL/min, and the column temperature was 40 °C.

Cell Transfections, Pull-Down of Recombinant Proteins, and Immunoblotting. HEK293 cells (ATCC collection) were cultured in DMEM containing 10% fetal bovine serum (FBS, Gibco) supplemented with 1% (v/v) antibiotic/antimycotic solution (Gibco). The cells were transiently transfected at 80% confluency in 6-well plates using pEBG2T plasmids coding for full length S6K[412E] and PKC ζ as GST-fusion proteins. In the S6K construct, the phosphorylatable residue Thr412 in the hydrophobic motif was mutated to glutamate in order to mimic a constitutive phosphorylation, which promotes interaction with the PDK1 PIF pocket. Transfections were performed using polyethylenimine (PEI, Polysciences Inc., USA), with a PEI/DNA ratio of 10:1 ($\mu\text{L}/\mu\text{g}$) and 2 μg of DNA per well. The cells were serum-starved during 24 h before treatment with compound 5h for 2 h. Then, IGF-I (10 ng/mL) was added for 20 min, and the cells were lysed. Isolation of the recombinant proteins was performed using glutathione sepharose essentially as described previously.³⁰ Aliquots of the isolates were resolved by sodium dodecyl sulfate polyacrylamide gel electrophoresis (SDS-PAGE), transferred to nitrocellulose membranes (Protan 0.2 μm , Whatman), and probed using phospho-specific antibodies: anti-phospho-S6K(Thr229) (cat. no. NSB918, Novus Biologicals) and anti-phospho-PKC ζ/λ (Thr410/403) (cat. no. 9378, Cell Signaling). To quantify the blotted amounts of the recombinant proteins, the membranes were also developed using an anti-GST antibody (cat. no. 2622, Cell Signaling). In another experiment, serum-starved HEK293 cells were treated with 5h for 2 h, followed by IGF-I stimulation (10 ng/mL) for 20 min. Lysates from the cells were subject to western blotting, and the blots were developed using phospho-specific antibodies: anti-phospho-S6(Ser235/236) (cat. no. 2211, Cell Signaling), which detects the phosphorylation specifically catalyzed by S6K on the ribosomal S6 protein, and anti-phospho-PKB(Thr308) (cat. no. 9275, Cell Signaling) which is specific for the PDK1-dependent T-loop phosphorylation of PKB. The quantified phosphorylation signals were normalized after reprobing the blots with anti-actin antibody (cat. no. A5441, Sigma–Aldrich).

Differential Scanning Fluorimetry. Protein unfolding was monitored by the increase in the fluorescence of the fluorophor SYPRO Orange (Invitrogen) using a realtime PCR device (StepOnePlus, Applied Biosystems) basically following the protocol described by Niesen et al.⁶⁰ PDK1 was diluted in 10 mM HEPES pH 7.5 buffer

containing 150 mM NaCl. Reactions were performed in a 10 μ L final volume in 96-well PCR microtiter plates (Greiner) and contained 1 μ M PDK1, 10 mM HEPES pH 7.5, 150 mM NaCl, 1/1000 SYPRO Orange, and 1 mM dithiothreitol. PIPtide or compounds (1% final DMSO concentration) were added to this reaction mixture. The temperature gradient was performed in steps of 0.3 $^{\circ}$ C in the range 25–70 $^{\circ}$ C. To calculate the midpoint temperature of transition (T_m) of PDK1 for each compound concentration, the data were exported to GraphPad Prism software, and the curves fitted to a Boltzmann sigmoidal equation with all $R^2 > 0.998$. Subtraction of the value obtained for the DMSO control (T_0) yielded ΔT_m values. Each ΔT_m data point reflected the average of a duplicate experiment. The ΔT_m values from different compound concentrations were then used to calculate EC_{50} values following to a dose–response curve fitting procedure embedded in Origin 8 software.

■ ASSOCIATED CONTENT

■ Supporting Information

Synthetic procedures and analytical data of compounds **0m**, **1a–g**, **1i–n**, **1p–v**, **2a–f**, **2i–n**, **2p–v**, **3m**, **4a–g**, **4i–n**, **4p–v**, **5a**, **5q**, **6a–d**, **6f**, **6g**, **6i**, **6k**, **6n**, **6q–s**, and **6u**; method for separation of **4h** into its enantiomers by HPLC including the analytical chromatograph. This material is available free of charge via the Internet at <http://pubs.acs.org>.

■ Accession Codes

The PDB code for **4h** complexed with PDK1 is 4AW1.

■ AUTHOR INFORMATION

■ Corresponding Author

*Phone: +49 681 302 70312; fax: +49 681 302 70308; e-mail: ma.engel@mx.uni-saarland.de.

■ Notes

The authors declare no competing financial interest.

■ ACKNOWLEDGMENTS

We thank Prof. Dr. R.W. Hartmann for generously providing lab facilities to the M.E. group and Prof. Dr. S. Zeuzem for his support of the R.M.B. lab. We acknowledge the support by the Deutsche Krebshilfe (106388) to R.M.B., by the Deutsche Forschungsgemeinschaft (DFG) (EN381/2-3) to M.E., and by the GoBio grant from the German Federal Ministry of Education and Science (0315102) to R.M.B. We are grateful to Michael Zender for his assistance with separation of the racemic compound **4h**.

■ ABBREVIATIONS USED

PDK1, phosphoinositide-dependent kinase-1; PI3, phosphatidylinositol-3; S6K, p70 S6 kinase; RSK, p90 ribosomal S6 kinase; SGK, serum- and glucocorticoid-induced protein kinase; PRK2, protein kinase C-related kinase 2; PIF, PRK2-interacting fragment; HM, hydrophobic motif; PH, pleckstrin homology; GST, glutathione-S-transferase; IRS, insulin receptor substrate; IGF, insulin-like growth factor

■ REFERENCES

- (1) Pearce, L. R.; Komander, D.; Alessi, D. R. The nuts and bolts of AGC protein kinases. *Nat. Rev. Mol. Cell Biol.* **2010**, *11*, 9–22.
- (2) Mora, A.; Komander, D.; van Aalten, D. M.; Alessi, D. R. PDK1, the master regulator of AGC kinase signal transduction. *Semin. Cell Dev. Biol.* **2004**, *15*, 161–170.
- (3) Bayascas, J. R.; Leslie, N. R.; Parsons, R.; Fleming, S.; Alessi, D. R. Hypomorphic mutation of PDK1 suppresses tumorigenesis in PTEN(\pm) mice. *Curr. Biol.* **2005**, *15*, 1839–1846.

- (4) Garcia-Echeverria, C.; Sellers, W. R. Drug discovery approaches targeting the PI3K/Akt pathway in cancer. *Oncogene* **2008**, *27*, 5511–5526.

- (5) Sato, S.; Fujita, N.; Tsuruo, T. Interference with PDK1-Akt survival signaling pathway by UCN-01 (7-hydroxystaurosporine). *Oncogene* **2002**, *21*, 1727–1738.

- (6) Zhu, J.; Huang, J. W.; Tseng, P. H.; Yang, Y. T.; Fowble, J.; Shiao, C. W.; Shaw, Y. J.; Kulp, S. K.; Chen, C. S. From the cyclooxygenase-2 inhibitor celecoxib to a novel class of 3-phosphoinositide-dependent protein kinase-1 inhibitors. *Cancer Res.* **2004**, *64*, 4309–4318.

- (7) Feldman, R. I.; Wu, J. M.; Polokoff, M. A.; Kochanny, M. J.; Dinter, H.; Zhu, D.; Biroc, S. L.; Alicko, B.; Bryant, J.; Yuan, S.; Buckman, B. O.; Lentz, D.; Ferrer, M.; Whitlow, M.; Adler, M.; Finster, S.; Chang, Z.; Arnaiz, D. O. Novel small molecule inhibitors of 3-phosphoinositide-dependent kinase-1. *J. Biol. Chem.* **2005**, *280*, 19867–19874.

- (8) Gopalsamy, A.; Shi, M.; Boschelli, D. H.; Williamson, R.; Olland, A.; Hu, Y.; Krishnamurthy, G.; Han, X.; Arndt, K.; Guo, B. Discovery of dibenzo[*c,f*][2,7]naphthyridines as potent and selective 3-phosphoinositide-dependent kinase-1 inhibitors. *J. Med. Chem.* **2007**, *50*, 5547–5549.

- (9) Islam, I.; Brown, G.; Bryant, J.; Hrvatin, P.; Kochanny, M. J.; Phillips, G. B.; Yuan, S.; Adler, M.; Whitlow, M.; Lentz, D.; Polokoff, M. A.; Wu, J.; Shen, J.; Walters, J.; Ho, E.; Subramanyam, B.; Zhu, D.; Feldman, R. I.; Arnaiz, D. O. Indolinone based phosphoinositide-dependent kinase-1 (PDK1) inhibitors. Part 2: optimization of BX-517. *Bioorg. Med. Chem. Lett.* **2007**, *17*, 3819–3825.

- (10) Peifer, C.; Alessi, D. R. Small-molecule inhibitors of PDK1. *ChemMedChem* **2008**, *3*, 1810–1838.

- (11) Nagashima, K.; Shumway, S. D.; Sathyanarayanan, S.; Chen, A. H.; Dolinski, B.; Xu, Y.; Keilhack, H.; Nguyen, T.; Wiznerowicz, M.; Li, L.; Lutterbach, B. A.; Chi, A.; Paweletz, C.; Allison, T.; Yan, Y.; Munshi, S. K.; Klippel, A.; Kraus, M.; Bobkova, E. V.; Deshmukh, S.; Xu, Z.; Mueller, U.; Szewczak, A. A.; Pan, B. S.; Richon, V.; Pollock, R.; Blume-Jensen, P.; Northrup, A.; Andersen, J. N. Genetic and pharmacological inhibition of PDK1 in cancer cells: characterization of a selective allosteric kinase inhibitor. *J. Biol. Chem.* **2011**, *286*, 6433–6448.

- (12) Copps, K. D.; White, M. F. Regulation of insulin sensitivity by serine/threonine phosphorylation of insulin receptor substrate proteins IRS1 and IRS2. *Diabetologia* **2012**, *55*, 2565–2582.

- (13) Bayascas, J. R.; Sakamoto, K.; Armit, L.; Arthur, J. S.; Alessi, D. R. Evaluation of approaches to generation of tissue-specific knock-in mice. *J. Biol. Chem.* **2006**, *281*, 28772–28781.

- (14) Um, S. H.; Frigerio, F.; Watanabe, M.; Picard, F.; Joaquin, M.; Sticker, M.; Fumagalli, S.; Allegrini, P. R.; Kozma, S. C.; Auwerx, J.; Thomas, G. Absence of S6K1 protects against age- and diet-induced obesity while enhancing insulin sensitivity. *Nature* **2004**, *431*, 200–205.

- (15) Um, S. H.; D'Alessio, D.; Thomas, G. Nutrient overload, insulin resistance, and ribosomal protein S6 kinase 1, S6K1. *Cell Metab.* **2006**, *3*, 393–402.

- (16) Sale, E. M.; Sale, G. J. Protein kinase B: signalling roles and therapeutic targeting. *Cell. Mol. Life Sci.* **2008**, *65*, 113–127.

- (17) Ellwood-Yen, K.; Keilhack, H.; Kunii, K.; Dolinski, B.; Connor, Y.; Hu, K.; Nagashima, K.; O'Hare, E.; Erkul, Y.; Di Bacco, A.; Gargano, D.; Shomer, N. H.; Angagaw, M.; Leccese, E.; Andrade, P.; Hurd, M.; Shin, M. K.; Vogt, T. F.; Northrup, A.; Bobkova, E. V.; Kasibhatla, S.; Bronson, R. T.; Scott, M. L.; Draetta, G.; Richon, V.; Kohl, N.; Blume-Jensen, P.; Andersen, J. N.; Kraus, M. PDK1 attenuation fails to prevent tumor formation in PTEN-deficient transgenic mouse models. *Cancer Res.* **2011**, *71*, 3052–3065.

- (18) Westmoreland, J. J.; Wang, Q.; Bouzaffour, M.; Baker, S. J.; Sosa-Pineda, B. Pdk1 activity controls proliferation, survival, and growth of developing pancreatic cells. *Dev. Biol.* **2009**, *334*, 285–298.

- (19) Biondi, R. M.; Cheung, P. C.; Casamayor, A.; Deak, M.; Currie, R. A.; Alessi, D. R. Identification of a pocket in the PDK1 kinase domain that interacts with PIF and the C-terminal residues of PKA. *EMBO J.* **2000**, *19*, 979–988.

- (20) Biondi, R. M.; Kieloch, A.; Currie, R. A.; Deak, M.; Alessi, D. R. The PIF-binding pocket in PDK1 is essential for activation of S6K and SGK, but not PKB. *EMBO J.* **2001**, *20*, 4380–4390.
- (21) Bogan, A. A.; Thorn, K. S. Anatomy of hot spots in protein interfaces. *J. Mol. Biol.* **1998**, *280*, 1–9.
- (22) Stephens, L.; Anderson, K.; Stokoe, D.; Erdjument-Bromage, H.; Painter, G. F.; Holmes, A. B.; Gaffney, P. R.; Reese, C. B.; McCormick, F.; Tempst, P.; Coadwell, J.; Hawkins, P. T. Protein kinase B kinases that mediate phosphatidylinositol 3,4,5-trisphosphate-dependent activation of protein kinase B. *Science* **1998**, *279*, 710–714.
- (23) Anderson, K. E.; Coadwell, J.; Stephens, L. R.; Hawkins, P. T. Translocation of PDK-1 to the plasma membrane is important in allowing PDK-1 to activate protein kinase B. *Curr. Biol.* **1998**, *8*, 684–691.
- (24) Beeson, M.; Sajan, M. P.; Dizon, M.; Grebenev, D.; Gomez-Daspert, J.; Miura, A.; Kanoh, Y.; Powe, J.; Bandyopadhyay, G.; Standaert, M. L.; Farese, R. V. Activation of protein kinase C-zeta by insulin and phosphatidylinositol-3,4,5-(PO4)3 is defective in muscle in type 2 diabetes and impaired glucose tolerance: amelioration by rosiglitazone and exercise. *Diabetes* **2003**, *52*, 1926–1934.
- (25) Farese, R. V.; Sajan, M. P.; Standaert, M. L. Insulin-sensitive protein kinases (atypical protein kinase C and protein kinase B/Akt): actions and defects in obesity and type II diabetes. *Exp. Biol. Med. (Maywood)* **2005**, *230*, 593–605.
- (26) Frojdo, S.; Vidal, H.; Piroola, L. Alterations of insulin signaling in type 2 diabetes: a review of the current evidence from humans. *Biochim. Biophys. Acta* **2009**, *1792*, 83–92.
- (27) Chou, M. M.; Hou, W.; Johnson, J.; Graham, L. K.; Lee, M. H.; Chen, C. S.; Newton, A. C.; Schaffhausen, B. S.; Toker, A. Regulation of protein kinase C ζ by PI 3-kinase and PDK-1. *Curr. Biol.* **1998**, *8*, 1069–1077.
- (28) Balendran, A.; Biondi, R. M.; Cheung, P. C.; Casamayor, A.; Deak, M.; Alessi, D. R. A 3-phosphoinositide-dependent protein kinase-1 (PDK1) docking site is required for the phosphorylation of protein kinase C ζ (PKC ζ) and PKC-related kinase 2 by PDK1. *J. Biol. Chem.* **2000**, *275*, 20806–20813.
- (29) Newton, A. C. Protein kinase C: poised to signal. *Am. J. Physiol. Endocrinol. Metab.* **2010**, *298*, E395–402.
- (30) Engel, M.; Hindie, V.; Lopez-Garcia, L. A.; Stroba, A.; Schaeffer, F.; Adrian, I.; Imig, J.; Idrissova, L.; Nastainczyk, W.; Zeuzem, S.; Alzari, P. M.; Hartmann, R. W.; Piiper, A.; Biondi, R. M. Allosteric activation of the protein kinase PDK1 with low molecular weight compounds. *EMBO J.* **2006**, *25*, 5469–5480.
- (31) Stroba, A.; Schaeffer, F.; Hindie, V.; Lopez-Garcia, L. A.; Adrian, I.; Fröhner, W.; Hartmann, R. W.; Biondi, R. M.; Engel, M. 3,5-Diphenylpent-2-enoic acids as allosteric activators of the protein kinase PDK1: Structure–activity relationships and thermodynamic characterisation of binding as paradigms for PIF-binding pocket-targeting compounds. *J. Med. Chem.* **2009**, *52*, 4683–4693.
- (32) Hindie, V.; Stroba, A.; Zhang, H.; Lopez-Garcia, L. A.; Idrissova, L.; Zeuzem, S.; Hirschberg, D.; Schaeffer, F.; Jorgensen, T. J.; Engel, M.; Alzari, P. M.; Biondi, R. M. Structure and allosteric effects of low-molecular-weight activators on the protein kinase PDK1. *Nat. Chem. Biol.* **2009**, *5*, 758–764.
- (33) Stockman, B. J.; Kothe, M.; Kohls, D.; Weibley, L.; Connolly, B. J.; Sheils, A. L.; Cao, Q.; Cheng, A. C.; Yang, L.; Kamath, A. V.; Ding, Y. H.; Charlton, M. E. Identification of allosteric PIF-pocket ligands for PDK1 using NMR-based fragment screening and ^1H - ^{15}N TROSY experiments. *Chem. Biol. Drug Des.* **2009**, *73*, 179–188.
- (34) Wei, L.; Gao, X.; Warne, R.; Hao, X.; Bussiere, D.; Gu, X. J.; Uno, T.; Liu, Y. Design and synthesis of benzoazepin-2-one analogues as allosteric binders targeting the PIF pocket of PDK1. *Bioorg. Med. Chem. Lett.* **2010**, *20*, 3897–3902.
- (35) Bobkova, E. V.; Weber, M. J.; Xu, Z.; Zhang, Y. L.; Jung, J.; Blume-Jensen, P.; Northrup, A.; Kunapuli, P.; Andersen, J. N.; Kariv, I. Discovery of PDK1 kinase inhibitors with a novel mechanism of action by ultrahigh throughput screening. *J. Biol. Chem.* **2010**, *285*, 18838–18846.
- (36) Sadowsky, J. D.; Burlingame, M. A.; Wolan, D. W.; McClendon, C. L.; Jacobson, M. P.; Wells, J. A. Turning a protein kinase on or off from a single allosteric site via disulfide trapping. *Proc. Natl. Acad. Sci. U.S.A.* **2011**, *108*, 6056–6061.
- (37) Dettori, R.; Sonzogni, S.; Meyer, L.; Lopez-Garcia, L. A.; Morrice, N. A.; Zeuzem, S.; Engel, M.; Piiper, A.; Neimanis, S.; Frodin, M.; Biondi, R. M. Regulation of the interaction between protein kinase C-related protein kinase 2 (PRK2) and its upstream kinase, 3-phosphoinositide-dependent protein kinase 1 (PDK1). *J. Biol. Chem.* **2009**, *284*, 30318–30327.
- (38) Xu, C.; Bartley, J. K.; Enache, D. I.; Knight, D. W.; Hutchings, G. J. High Surface Area MgO as a Highly Effective Heterogeneous Base Catalyst for Michael Addition and Knoevenagel Condensation Reactions. *Synthesis* **2005**, *19*, 3468–3476.
- (39) Ma, S.; Yu, S.; Yin, S. Studies on K_2CO_3 -catalyzed 1,4-addition of 1,2-allenic ketones with diethyl malonate: controlled selective synthesis of beta,gamma-unsaturated enones and α -pyrones. *J. Org. Chem.* **2003**, *68*, 8996–9002.
- (40) Ma, S.; Yin, S.; Li, L.; Tao, F. K_2CO_3 -catalyzed Michael addition–lactonization reaction of 1,2-allenyl ketones with electron-withdrawing group substituted acetates. An efficient synthesis of α -pyrone derivatives. *Org. Lett.* **2002**, *4*, 505–507.
- (41) March, J. The decarboxylation of organic acids. *J. Chem. Educ.* **1963**, *40*, 212–213.
- (42) Ni, J.; Auston, D. A.; Freilich, D. A.; Muralidharan, S.; Sobie, E. A.; Kao, J. P. Photochemical gating of intracellular Ca^{2+} release channels. *J. Am. Chem. Soc.* **2007**, *129*, 5316–5317.
- (43) Mai, A.; Cheng, D.; Bedford, M. T.; Valente, S.; Nebbioso, A.; Perrone, A.; Brosch, G.; Sbardella, G.; De Bellis, F.; Miceli, M.; Altucci, L. Epigenetic multiple ligands: mixed histone/protein methyltransferase, acetyltransferase, and class III deacetylase (sirtuin) inhibitors. *J. Med. Chem.* **2008**, *51*, 2279–2290.
- (44) Busschots, K.; Lopez-Garcia, L. A.; Lammi, C.; Stroba, A.; Zeuzem, S.; Piiper, A.; Alzari, P. M.; Neimanis, S.; Arencibia, J. M.; Engel, M.; Schulze, J. O.; Biondi, R. M. Substrate-selective inhibition of protein kinase PDK1 by small compounds that bind to the PIF-pocket allosteric docking site. *Chem. Biol.* **2012**, in press.
- (45) Lu, Y.; Shi, T.; Wang, Y.; Yang, H.; Yan, X.; Luo, X.; Jiang, H.; Zhu, W. Halogen bonding—a novel interaction for rational drug design? *J. Med. Chem.* **2009**, *52*, 2854–2862.
- (46) Fröhner, W.; Lopez-Garcia, L. A.; Neimanis, S.; Weber, N.; Navratil, J.; Maurer, F.; Stroba, A.; Zhang, H.; Biondi, R. M.; Engel, M. 4-Benzimidazolyl-3-phenylbutanoic acids as novel PIF-pocket-targeting allosteric inhibitors of protein kinase PKC ζ . *J. Med. Chem.* **2011**, *54*, 6714–6723.
- (47) Lopez-Garcia, L. A.; Schulze, J. O.; Fröhner, W.; Zhang, H.; Süß, E.; Weber, N.; Navratil, J.; Amon, S.; Hindie, V.; Zeuzem, S.; Jorgensen, T. J. D.; Alzari, P. M.; Neimanis, S.; Engel, M.; Biondi, R. M. Allosteric regulation of protein kinase PKC ζ by the N-terminal C1 domain and small compounds to the PIF-pocket. *Chem. Biol.* **2011**, *18*, 1463–1473.
- (48) Olsen, J. A.; Banner, D. W.; Seiler, P.; Obst Sander, U.; D'Arcy, A.; Stihle, M.; Muller, K.; Diederich, F. A fluorine scan of thrombin inhibitors to map the fluorophilicity/fluorophobicity of an enzyme active site: evidence for C–F \cdots C=O interactions. *Angew. Chem., Int. Ed.* **2003**, *42*, 2507–2511.
- (49) Niimi, T.; Orita, M.; Okazawa-Igarashi, M.; Sakashita, H.; Kikuchi, K.; Ball, E.; Ichikawa, A.; Yamagiwa, Y.; Sakamoto, S.; Tanaka, A.; Tsukamoto, S.; Fujita, S.; Tatsuta, K.; Maeda, Y.; Chikachi, K. Design and synthesis of non-peptidic inhibitors for the Syk C-terminal SH2 domain based on structure-based in-silico screening. *J. Med. Chem.* **2001**, *44*, 4737–4740.
- (50) Gao, Y.; Luo, J.; Yao, Z. J.; Guo, R.; Zou, H.; Kelley, J.; Voigt, J. H.; Yang, D.; Burke, T. R., Jr. Inhibition of Grb2 SH2 domain binding by non-phosphate-containing ligands. 2. 4-(2-Malonyl)phenylalanine as a potent phosphotyrosyl mimetic. *J. Med. Chem.* **2000**, *43*, 911–920.
- (51) Fedorov, O.; Marsden, B.; Pogacic, V.; Rellos, P.; Muller, S.; Bullock, A. N.; Schwaller, J.; Sundstrom, M.; Knapp, S. A systematic

interaction map of validated kinase inhibitors with Ser/Thr kinases. *Proc. Natl. Acad. Sci. U.S.A.* **2007**, *104*, 20523–20528.

(52) Kroe, R. R.; Regan, J.; Proto, A.; Peet, G. W.; Roy, T.; Landro, L. D.; Fuschetto, N. G.; Pargellis, C. A.; Ingraham, R. H. Thermal denaturation: a method to rank slow binding, high-affinity P38 α MAP kinase inhibitors. *J. Med. Chem.* **2003**, *46*, 4669–4675.

(53) Jansen, A. B.; Russell, T. J. Some novel penicillin derivatives. *J. Chem. Soc.* **1965**, *65*, 2127–2132.

(54) Daehne, W.; Frederiksen, E.; Gundersen, E.; Lund, F.; Morch, P.; Petersen, H. J.; Roholt, K.; Tybring, L.; Godtfredsen, W. O. Acyloxymethyl esters of ampicillin. *J. Med. Chem.* **1970**, *13*, 607–612.

(55) Ferres, H. Prodrugs of beta-lactam antibiotics. *Drugs Today* **1983**, *19*, 499–538.

(56) Bundgaard, H.; Nielsen, N. M. Esters of *N,N*-disubstituted 2-hydroxyacetamides as a novel highly biolabile prodrug type for carboxylic acid agents. *J. Med. Chem.* **1987**, *30*, 451–454.

(57) D'Arezzo, S.; Incerpi, S.; Davis, F. B.; Acconcia, F.; Marino, M.; Farias, R. N.; Davis, P. J. Rapid nongenomic effects of 3,5,3'-triiodo-L-thyronine on the intracellular pH of L-6 myoblasts are mediated by intracellular calcium mobilization and kinase pathways. *Endocrinology* **2004**, *145*, 5694–5703.

(58) James, A. M.; Wei, Y. H.; Pang, C. Y.; Murphy, M. P. Altered mitochondrial function in fibroblasts containing MELAS or MERRF mitochondrial DNA mutations. *Biochem. J.* **1996**, *318* (Pt 2), 401–407.

(59) Zamecnik, P.; Aghajanian, J.; Zamecnik, M.; Goodchild, J.; Witman, G. Electron micrographic studies of transport of oligodeoxynucleotides across eukaryotic cell membranes. *Proc. Natl. Acad. Sci. U.S.A.* **1994**, *91*, 3156–3160.

(60) Niesen, F. H.; Berglund, H.; Vedadi, M. The use of differential scanning fluorimetry to detect ligand interactions that promote protein stability. *Nat. Protoc.* **2007**, *2*, 2212–2221.